*Human Molecular Genetics, 2014, Vol. 23, No. 10* **2711–2720**
*doi:10.1093/hmg/ddt664*
*Advance Access published on January 16, 2014*

# An etiologic regulatory mutation in *IRF6* with loss- and gain-of-function effects

**Walid D. Fakhouri[1,†], Fedik Rahimov[4,‡], Catia Attanasio[5], Evelyn N. Kouwenhoven[6], Renata L. Ferreira De Lima[4], Temis Maria Felix[8], Larissa Nitschke[1], David Huver[1], Julie Barrons[1], Youssef A. Kousa[2], Elizabeth Leslie[4], Len A. Pennacchio[5], Hans Van Bokhoven[6,7], Axel Visel[5], Huiqing Zhou[6,9], Jeffrey C. Murray[4] and Brian C. Schutte[1,3,*]**

[1]Microbiology and Molecular Genetics, [2]Department of Biochemistry and Molecular Biology and [3]Department of Pediatrics and Human Development, Michigan State University, East Lansing, MI 48824, USA [4]Department of Pediatrics, The University of Iowa, Iowa City, IA 52242, USA [5]Genomics Division, Lawrence Berkeley National Laboratory, Berkeley, CA 94720, USA [6]Department of Human Genetics, Nijmegen Centre for Molecular Life Sciences and [7]Department of Cognitive Neuroscience, Donders Institute for Brain, Cognition, and Behavior, Radboud University Medical Centre, Nijmegen, The Netherlands [8]Medical Genetics Service, Hospital de Clinicas de Porto Alegre, Porto Alegre, Brazil [9]Faculty of Science, Department of Molecular Developmental Biology, Radboud University Nijmegen, Nijmegen, The Netherlands

Received September 25, 2013; Revised December 7, 2013; Accepted December 23, 2013

**DNA variation in *Interferon Regulatory Factor 6* (*IRF6*) causes Van der Woude syndrome (VWS), the most common syndromic form of cleft lip and palate (CLP). However, an etiologic variant in *IRF6* has been found in only 70% of VWS families. To test whether DNA variants in regulatory elements cause VWS, we sequenced three conserved elements near *IRF6* in 70 VWS families that lack an etiologic mutation within *IRF6* exons. A rare mutation (*350dupA*) was found in a conserved *IRF6* enhancer element (*MCS9.7*) in a Brazilian family. The *350dupA* mutation abrogated the binding of p63 and E47 transcription factors to cis-overlapping motifs, and significantly disrupted enhancer activity in human cell cultures. Moreover, using a transgenic assay in mice, the *350dupA* mutation disrupted the activation of *MCS9.7* enhancer element and led to failure of *lacZ* expression in all head and neck pharyngeal arches. Interestingly, disruption of the p63 Motif1 and/or E47 binding sites by nucleotide substitution did not fully recapitulate the effect of the *350dupA* mutation. Rather, we recognized that the *350dupA* created a CAAAGT motif, a binding site for Lef1 protein. We showed that Lef1 binds to the mutated site and that overexpression of Lef1/β-Catenin chimeric protein repressed *MCS9.7-350dupA* enhancer activity. In conclusion, our data strongly suggest that *350dupA* variant is an etiologic mutation in VWS patients and disrupts enhancer activity by a loss- and gain-of-function mechanism, and thus support the rationale for additional screening for regulatory mutations in patients with CLP.**

## INTRODUCTION

Cleft lip and palate (CLP) is one of the most common birth defects in humans with a frequency of 1/700 live births (1). DNA variation in *Interferon Regulatory Factor 6* (*IRF6*) causes Van der Woude syndrome (VWS), the most common syndromic form of CLP, and contributes 12% of the risk for non-syndromic CLP worldwide (2,3). VWS is an autosomal dominant genetic disorder characterized by a highly, but incompletely, penetrant (92%) phenotype of lip pits in lower lip and CLP (4). To date, etiologic *IRF6* variants have been found in ~70% of families with VWS (2,5,6). The etiologic mutations in the remaining 30% of VWS families could be located in regulatory elements around *IRF6*, in other causative genes, or were missed due to sequencing

*To whom correspondence should be addressed at: 5162 Biomedical and Physical Science Building, Microbiology and Molecular Genetics, Michigan State University, East Lansing, MI 48823, USA. Tel: +1 5178845346; Fax: +1 5173538957; Email: schutteb@msu.edu
†Present address: Department of Diagnostic and Biomedical Sciences, School of Dentistry, University of Texas Health Science Center, Houston, TX 77054, USA.
‡Present address: Program in Genomics, Division of Genetics, Boston Children's Hospital, Harvard Medical School, Boston, MA 02115, USA.

limitations (e.g. large genomic deletions). Previous studies suggested that mutations at other loci and large deletions at the *IRF6* locus account for a small fraction of missing mutations (7,8). Thus, we hypothesized that VWS-causing mutations can be found in regulatory elements around *IRF6*.

Our previous *in vivo* studies identified *MCS9.7* as a regulatory element for *IRF6* (9). *MCS9.*7 is a 607 bp multi-species conserved sequence that is located 9.7 kb upstream from the *IRF6* transcriptional start site, and displayed enhancer activity in a transgenic *in vivo* murine assay (9). Recently, we showed that the *MCS9.7* enhancer activity recapitulated the endogenous expression of *Irf6* in nearly all tissues during orofacial development (10). *MCS9.7* was shown to be clinically relevant because it contains rs642961, a common DNA variant that is highly associated with non-syndromic CLP (9). However, rs642961 did not account for all of the risk at the *IRF6* locus. Thus, these data support the hypothesis that additional disease-associated variants can be found in *MCS9.7* and in other multi-species conserved sequences near *IRF6*.

Recent studies linked regulation of *IRF6* expression to p63 (11), the transcription factor encoded by *TP63*. Like *IRF6*, *TP63* is required for development of the lip and palate in humans and mice (12–15). In humans, *IRF6* expression was reduced in regenerated human epidermal tissues obtained from patients carrying a dominant-negative allele of *TP63* (16). In mice, embryos that lacked p63 (11) or had reduced p63 expression (17) showed a decrease in Irf6 expression. Moreover, a genome-wide profile of p63 binding showed that a strong p63 binding signal mapped to *MCS9.7* (11,18,19). Finally, molecular studies in human primary keratinocytes showed that *MCS9.7* actually contains two binding sites for p63, Motif1 and Motif2, which are 60 bp apart. Importantly, abolishing both Motif1 and Motif2 significantly reduced *MCS9.7* enhancer activity, whereas abolishing either motif separately reduced, but did not disrupt, enhancer activity (11). In sum, these data provide strong evidence that p63 regulates *IRF6* expression by directly binding to two neighboring sites within *MCS9.7*.

While mutations in regulatory elements have been associated with human genetic disorders, few of these regulatory mutations led to genetic disorders by a gain-of-function mechanism (20–23). In this study, we sequenced the *MCS9.7* enhancer element and two other conserved regions in 70 families with VWS that lack exonic mutations within *IRF6*. We found a single nucleotide duplication within the *MCS9.7* enhancer in three affected family members. Surprisingly, while this DNA variant disrupted p63 Motif1 only, it abrogated *in vitro* and *in vivo MCS9.7* enhancer activity. To understand this observation, we tested the hypothesis that this rare variant abolishes *MCS9.*7 enhancer activity by a mechanism that includes both a loss- and gain-of-function effects.

## RESULTS

### Mapping a rare mutation in a VWS pedigree

To search for mutations in regulatory elements, we sequenced three highly conserved regions at the *IRF6* locus (Fig. 1A) in 70 probands of VWS families that lack exonic mutations in *IRF6*. The three regions included *MCS9.7*, a previously identified enhancer element for *IRF6*, located 9.7 kb upstream of the transcriptional start site (9,10). We identified one rare DNA variant, a duplicated Adenosine (A) nucleotide at position 350 within the *MCS9.7* enhancer (*350dupA*) (Fig. 1B). The *350dupA* mutation was identified in a Brazilian pedigree with three generations (Fig. 1C). Three affected individuals in this pedigree have lip pits, a hallmark of VWS (Fig. 1D). We obtained a DNA sample from five individuals. All five had the *350dupA* mutation, including two individuals that were unaffected. However, *350dupA* was not found in 100 unaffected controls nor in the 1092 genomes sampled from 14 populations in the NHLBI/ESP database (www.eversusgs.washington.edu/EVS). In addition, the sequence around the *350dupA* mutation is highly conserved in 10 vertebrates (Fig. 1E), which suggests a functional role for this sequence. Surprisingly, a motif prediction program indicated that the *350dupA* mutation is located in the middle of two overlapping cis motifs, a p63 and an Ebox motif (Fig. 1F). Importantly, there is one other predicted p63 and three other Ebox motifs in the *MCS9.7* element, designated as p63 Motif1 and Motif2 (11) and Ebox1-4, respectively (Supplementary Material, Table S1). The *350dupA* mutation is predicted to disrupt p63 Motif1 and Ebox3 (Fig. 1F). In addition, sequence analysis of *MCS9.7* enhancer element showed that all five individuals in the Brazil family did not carry the risk allele at rs642961.

### Disruption of *MCS9.7* enhancer activity by *350dupA* mutation

To test the effect of the *350dupA* mutation on *MCS9.7* enhancer activity, we performed transient transfection assays in human embryonic epithelial kidney (HEK293) cells. While the *MCS9.7* element increased luciferase activity 11-fold compared with the basic plasmid, the *MCS9.7* element with the *350dupA* mutation reduced the enhancer activity nearly to the control level (Fig. 2A). To confirm the effect of the *350dupA* mutation under *in vivo* conditions, we performed transgenic analysis on murine embryos using the same wild-type and mutant enhancer elements. As shown previously, transgenic embryos that carried the wild-type *MCS9.7* element had *LacZ* expression in orofacial tissues, in particular, the lambdoid junction where the maxillary, lateral nasal and medial nasal prominences fuse to form the lip (Fig. 2B). However, transgenic embryos that carried the *MCS9.7* element with the *350dupA* mutation had no *LacZ* expression. To quantify this observation, we compared 15 embryos that carried *MCS9.7-LacZ* with 16 transgenic embryos that carried *MCS9.7-350dupA-LacZ*. While 8/15 embryos with wild-type *MCS9.7* showed a reproducible staining in craniofacial tissues, only 1/16 transgenic embryo with the *MCS9.7-350dupA* allele showed weak staining (Fig. 2C). Surprisingly, while the *350dupA* rare mutation disrupted *MCS9.7* enhancer activity *in vivo*, the common risk mutation rs642961 that is highly associated with the common form of CLP had no detectable effect on enhancer activity using a similar murine transgenic assay (Supplementary Material, Fig. S1).

### Effect of *350dupA* on binding of transcription factors to *MCS9.7* enhancer element

First, since the *350dupA* mutation is within cis-overlapping sites for p63 Motif1 and Ebox3/4, we tested whether p63 and bHLH transcription factors bind to *MCS9.7* element under normal cellular

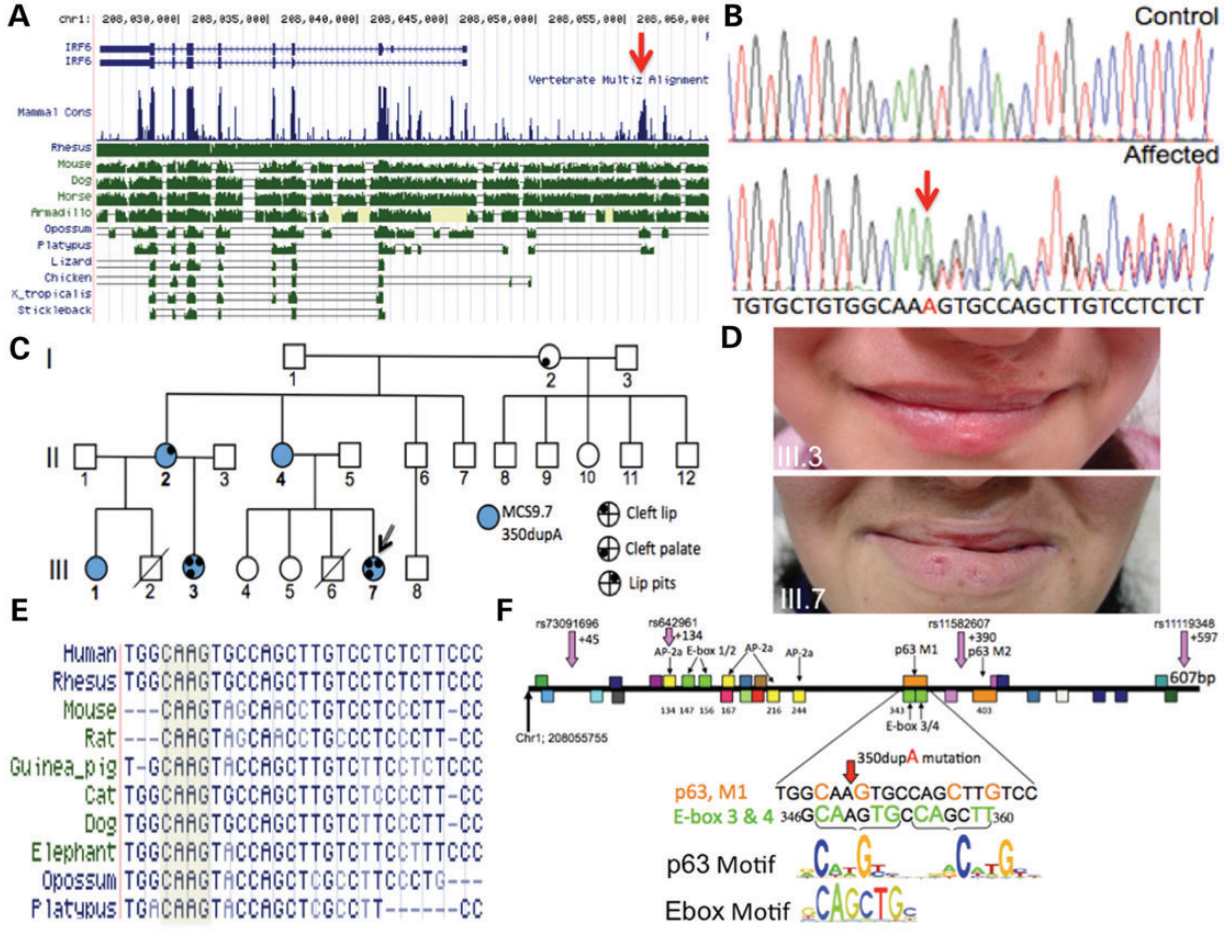


**Figure 1.** A Rare mutation mapped in *IRF6* enhancer element. (**A**) A screen shot from UCSC Genome Browser that shows *IRF6* coding and highly conserved regions. Exons 1–9 are connected rectangles from right to left. The track below is the multi-species conservation, and includes *MCS9.7* enhancer element located 9.7 kb upstream of exon 1. The green tracks are the multi-species conservation in eleven vertebrates. (**B**) The chromatograph of the DNA sequence from unaffected and affected individuals from the Brazilian family. The red arrow indicates the position of the duplicated A nucleotide. (**C**) Pedigree of a Brazilian family with Van der Woude syndrome (VWS). DNA samples were collected from five individuals (II.2, II.4, III.1, III.3 and III.7). All carried the *MCS9.7-350dupA* variant (blue circle). (**D**) Digital photos of two affected patients showing pits (III.3) and bi-lateral pits (III.7) in lower lip and repaired cleft lip in both. (**E**) The nucleotide conservation of the cis-overlapping motifs of Ebox 3 and 4 and p63 Motif 1. (**F**) Diagram of *MCS9.7* element shows the binding sites of AP2a (yellow box), p63 Motif 1 and Motif 2 (orange box) and Ebox motifs (grey box). The rest of the colored boxes represent putative binding sites of transcription factors that expressed or have a known role in orofacial clefting (Supplementary Material, Table S1). Below the diagram of *MCS9.7* is the sequence of the cis-overlapping p63 Motif 1 and Ebox 3 and 4 Motifs. The position of the A duplication mutation is shown by the vertical red arrow. A Logo representation of p63 motif and Ebox motif (jaspar.genereg.net).

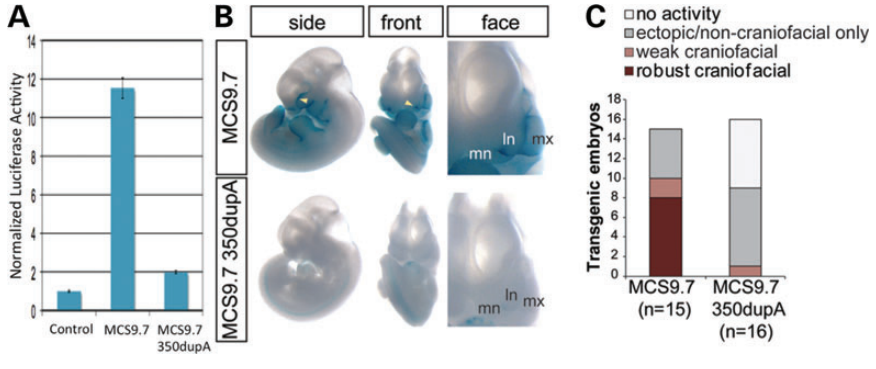


**Figure 2.** The effect of the *350dupA* mutation on *MCS9.7* enhancer activity. (**A**) HEK293 cells were transfected with three different constructs, no enhancer (Control), *MCS9.7* enhancer (*MCS9.7*) and *MCS9.7* enhancer with *350dupA* mutation (*MCS9.7-350dupA*). Luciferase activity was measured 24 h post-transfection and normalized to internal Renilla activity. (**B**) *In vivo* enhancer activity of *MCS9.7* from E11.5 transgenic embryos and *MCS9.7* with the *350dupA* mutation (*MCS-9.7*-350dupA). Reproducible craniofacial staining was observed at the pharyngeal arches and the lambdoid structure (yellow arrow; fusion site of the lateral nasal (ln), medial nasal (mn) and maxillary (mx) prominences). (**C**) Annotation of *MCS9.7* and *MCS9.7*-350dupA enhancer activity patterns. Embryos were classified into four categories of patterns: (i) no LacZ staining detected (white), (ii) non-craniofacial (ectopic) LacZ activity (gray), (iii) weak craniofacial LacZ activity as in *MCS9.7* representative embryo (pink), (iv) strong craniofacial LacZ activity, pattern as *MCS9.7* representative embryo (red). The data in each column are represented as the mean of five replicates ± SD.

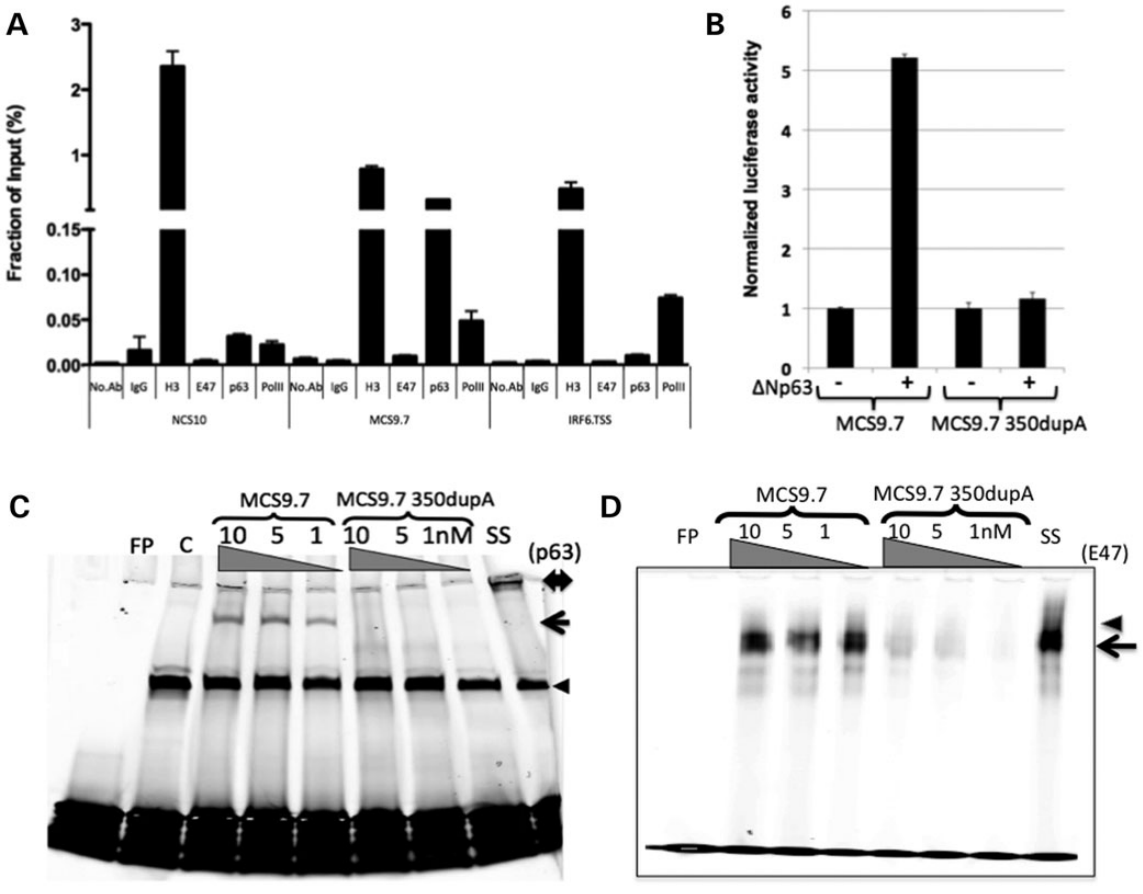


**Figure 3.** Effect of *350dupA* mutation on transcription factor binding to *MCS9.7*. (**A**) Chromatin immunoprecipitation from HaCaT cells followed by quantitative real-time PCR was used to detect binding of indicated transcription factors to *MCS9.7* enhancer element, to the non-conserved sequence element (*NCS10*) that is 800 bp away from *MCS9.7*, and at the transcriptional start site for *IRF6* (*IRF6* TSS). (**B**) The effect of the 350*dupA* mutation on the *MCS9.7* enhancer activity was tested before (−) and after (+) transactivation with ΔNp63 expression vector. Sosa2 cells were transfected with indicated luciferase construct in comparison with cotransfection of these plasmids with ΔNp63 expression vector. (**C**) EMSA assay was used to test the effect of *350dupA* mutation on the binding of p63 protein to Motif 1. A unique shift band (arrow) in ascending concentrations of recombinant p63 protein was observed (arrow) compare with free probe alone and probe with only reticulocyte extract mixture (arrowhead). The *350dupA* mutation completely disrupts p63 protein binding. The binding of p63 was confirmed by using monoclonal antibodies against p63 protein shown by the super shift band (double head arrow). (**D**) Binding of E47 to *MCS9.7* probe using a dilution series of E47 protein. Recombinant E47 protein showed a unique shift band (arrow) when incubated with wild-type probe compare with free probe alone (FP). The binding of E47 to *MSC9.7-350dupA* was abolished in all three ascending concentrations. The specificity of E47 binding was confirmed using antibodies against E47 proteins shown by the super shift band (head arrow). The data in each column are represented as the mean of five replicates ± SD.

conditions using keratinocytes from adult human skin (HaCaT). As previously observed (11), we detected strong binding of p63 within *MCS9.7* by chromatin immunoprecipitation (ChIP) followed by qPCR, and only a weak signal was observed within a nearby non-conserved region, indicating the specificity of the binding to *MCS9.7* element (Fig. 3A). For the Ebox sites, we tested binding with two bHLH transcription factors, E47 and cMYC, whose expression patterns overlap with Irf6 in the orofacial epithelium (24). We detected a minor signal for E47 within *MCS9.7* compared with controls (a non-specific IgG and a no antibody control) (Fig. 3A). Using human embryonic epithelial kidney cells (HEK293), we detected a strong binding of the cMYC protein within *MCS9.7* element (Supplementary Material, Fig. S2). We also observed a strong signal by ChIP for PolII protein at the promoter region of *IRF6* as an indicator of transcriptional activity. Interestingly, we detected a strong ChIP signal for PolII at the *MCS9.7* enhancer element too, suggesting a looping of the element despite nearly 10 Kb of intervening DNA sequence (Fig. 3A).

An EMSA was used to test the effect of the *350dupA* mutation on binding of p63 and E47 to the cis-overlapping motif within the *MCS9.7* enhancer element. Using increasing concentrations of recombinant p63 protein, we observed a unique shifting band (Fig. 3C). However, the *350dupA* mutation abolished p63 binding. Using a monoclonal antibody against p63 protein, we observed a super shift band, confirming the specificity of p63 binding to the wild-type probe (Fig. 3C). Similarly, EMSA results showed that recombinant E47 protein bound to the overlapping Ebox3/4 sites, located within the same DNA probe as p63 Motif1 (Fig. 3D). However, *350dupA* mutation disrupted the binding of E47 recombinant protein. The specificity of the binding was confirmed with the super shift band using antibodies against E47 protein and also by running a competitive inhibitory assay using excess of unlabeled wild-type probe that abolished E47 binding. However, addition of excess *MSC9.7-350dupA* or a random non-specific probe did not interfere with the binding (Supplementary Material, Fig. S3).

### Overexpression of p63 is not sufficient for compensation

Since the *350dupA* mutation disrupted p63 Motif1 but not Motif2, we hypothesized that overexpression of p63 would compensate for the loss of binding to Motif1 by saturating the binding to Motif2. Using human osteosarcoma (Soas2) cells that lack endogenous expression of p63 protein, we co-transfected these cells with an expression vector for ΔNp63 and a luciferase plasmid driven by the wild-type *MCS9.7* enhancer or by the *MCS9.7-350dupA* mutant enhancer. Overexpression of ΔNp63 significantly increased luciferase activity by 6-fold compared with control cells without ΔNp63 vector (Fig. 3B). However, luciferase activity was not induced when the *MCS9.7-350dupA* enhancer element was used (Fig. 3B). We concluded that overexpression of p63 was not sufficient to compensate for the *350dupA* mutation, despite the presence of Motif2.

### Disruption of the p63 Motif1 and Ebox3/4 sites individually do not mimic the *350dupA* effect

Since the *350dupA* mutation abrogated binding by both p63 and bHLH factors, it was not clear which factor was most important for *MCS9.7* enhancer activity. To distinguish between these possibilities, we independently mutated the p63 Motif1 and the Ebox3/4 sites and measured *MCS9.7* enhancer activity in HEK293 cells. In comparison with the wild-type *MCS9.7* enhancer (M1/E3E4), the *MCS9.7-350dupA* element (A(m1/e3)E4) decreased the activity ∼5-fold (Fig. 4). However, disruption of the p63 Motif1 without affecting Ebox3/4 (m1/E3E4) reduced the luciferase activity by only 1.3-fold, and disruption of Ebox3 and 4 without affecting p63 Motif1 (M1/e3e4) showed a slight increase in activity (Fig. 4). To test whether the *350dupA* effect was due to an insertion mutation, we inserted an Adenosine nucleotide in the spacer between Ebox3 and Ebox4 (M1/E3AE4), and we inserted a C nucleotide (C(m1/e3)E4) in the exact position of the *350dupA* mutation. Only the C insertion had a negative effect, but it was similar to the loss of the p63 Motif1 site (Fig. 4). In addition, we tested whether insertion and substitution together would disrupt enhancer activity. To do that, we disrupted p63 Motif1 by substitution and insertion of T nucleotide (m1/E3E4T), and also disrupted Ebox3/4 by substitution and p63 Motif1 by insertion of T nucleotide (m1/e3e4T). Although the construct (m1/e3e4T) was the most disruptive to luciferase activity compared with other mutated constructs, it was not sufficient to mimic *350dupA* effect (Fig. 4). Collectively, our results showed that while the p63 Motif1 site is important for *MCS9.7* activity, nucleotide substitution and insertion mutations were not sufficient to replicate the effects of the *350dupA* mutation.

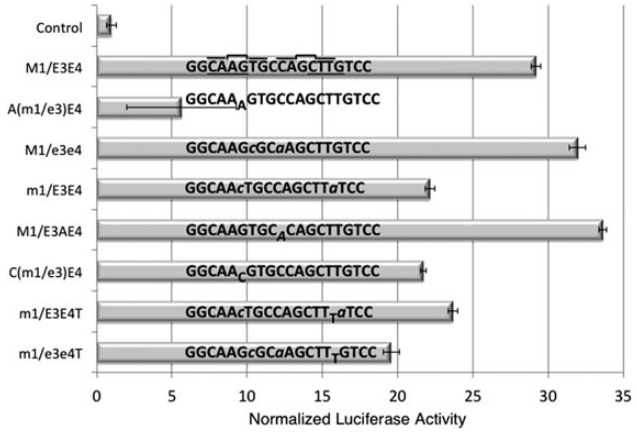


**Figure 4.** Allelic Architecture of *350dupA* Mutation within a cis-overlapping Motif. Substitution (lowercase, *italic*) and insertion (subscript) mutations were made in *MCS9.7* to delineate effects on P63 motif1 (M1), Ebox 3 (E3) and Ebox 4 (E4) in HEK293 cells. The construct without *MCS9.7* enhancer was used as base line control. The common-type *MCS9.7* enhancer (M1/E3E4) increased luciferase activity 29-fold, whereas *350dupA* mutation (A(m1/e3)E4) decreased the activity by 6-fold compared with the common sequence of *MCS9.7*. Disruption of Ebox 3 and 4 (M1/e3e4) did not change the luciferase activity, while abolishing only P63 motif1 (m1/E3E4) reduced the luciferase activity by 22%. Insertion of A nucleotide in the spacer between Ebox 3 and 4 (M1/E3AE4) slightly increased luciferase activity, while the insertion of C nucleotide (C(m1e3)E4) in the same position similar to *350dupA* reduced the activity by 25%. Disruption of P63 Motif1 and insertion of T nucleotide (m1/E3E4T) reduced activity by 18%; however, disruption of P63 Motif 1, Ebox 3 and 4 and insertion of T nucleotide (m1/e3e4T) to create a CAAAG motif decreased the luciferase activity by 35%.

### The *350dupA* mutation creates a *de novo* Lef1 binding site

Since mutating both or either p63 Motif1 and/or Ebox 3/4 was not sufficient to replicate the *350dupA* mutation, we hypothesized that the *350dupA* mutation had a gain-of-function activity by creating a *de novo* binding site for a repressor. The *350dupA* mutation creates a CAAAG motif, a putative binding site for TCF4/Lef1 protein. To test whether the 3*50dupA* mutation alters binding by Lef1, we performed EMSA using recombinant Lef1 protein. We observed that Lef1 protein weakly bound to the wild-type *MCS9.7* probe, but more strongly to *MCS9.7-350dupA* (Fig. 5A). The specificity of Lef1 binding to both probes was confirmed by a supershift using an antibody against Lef1 protein. To test whether the *350dupA* altered Lef1-mediated repression of *MCS9.7* enhancer activity, we measured wild-type and mutant *MCS9.7* enhancer activity in HEK293 cells that overexpressed a Lef1-βCat chimera construct. Wild-type *MCS9.7* activity was reduced 1.2-fold when Lef1-βCat protein was overexpressed, while the activity of the *MCS9.7-350dupA* construct was reduced by 2-fold (Fig. 5B). Further, we observed that Lef1 was co-expressed with Irf6 in the oral epidermis during embryonic development (Fig. 5C–E). Thus, Lef1 is present in cells where Irf6 was expressed and *MCS9.7* was active (10). Also, Wnt signaling was previously shown to be present and even necessary for proper development of the lip (17). These data are consistent with the hypothesis that the *350dupA* mutation altered *MCS9.7* enhancer activity through a gain-of-function mechanism mediated by Lef1.

In sum, we propose the following model to explain how the human *350dupA* mutation in Motif1 had the same effect on *MCS9.7* enhancer activity as *in vitro* disruption of both Motif1 and Motif2 in the earlier study (11). We propose that the *350dupA* mutation inhibits *MCS9.7* enhancer activity by; (i) a loss-of-function mechanism by abrogating binding of p63 protein at Motif1, and (ii) a gain-of-function mechanism by creating a *de novo* binding site for a repressive protein complex that abrogated binding of p63 protein at Motif2 through an as yet unknown interaction (Fig. 6).

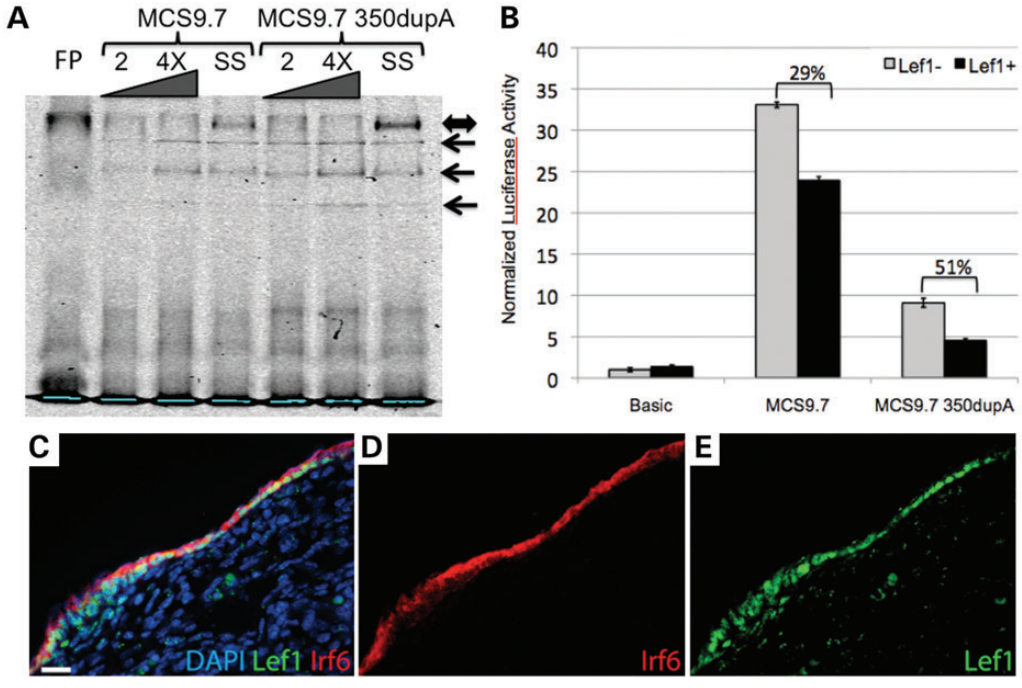


**Figure 5.** *350DupA* mutation creates a novel binding site. (**A**) EMSA assay showed unique shift bands when *MCS9.7* and *MCS9.7-350dupA* probes incubated with Lef1 recombinant protein. The binding specificity of Lef1 protein was confirmed using polyclonal antibodies against Lef1 as shown with the super shift (SS) bands when *MCS9.7* and *MCS9.7-350dupA* probes were incubated with Lef1 protein and anti-Lef1 antibodies. The *350dupA* mutation creates a novel Lef1 binding site. (**B**) Basic construct without *MCS9.7* element showed a minimal luciferase activity, while *MCS9.7* enhancer element increased luciferase activity 33-fold. The *350dupA* mutation reduced the activity about 4-fold compared *MCS9.7*. Cotransfection with the Lef1-βCatenin expression vector did not change luciferase activity in basic construct but reduced the activity by 29% when driven by *MCS9.7*. Interestingly, luciferase activity driven by *MCS9.7-350dupA* was significantly reduced by 51% when cotransfected with Lef1-βCatenin vector. (**C**) A merge image of red and green fluorescent staining shows that both Irf6 and Lef1 are colocalized in the same epidermal cells. A pre-merged immuno-staining shows the expression of Irf6 in red fluorescent (**D**) and Lef1 in green fluorescent (**E**) in the epidermis of murine embryo at E14.5.

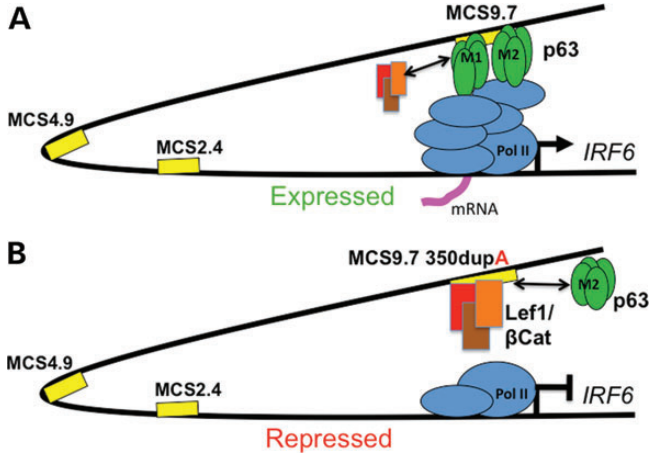


**Figure 6.** A working model for the *350dupA* mutation in patients with Van der Woude syndrome. (**A**) In normal situation, p63 protein binds to Motif1 (M1) and 2 (M2) which are 60 bp apart within *MCS9.7* enhancer element and drives *IRF6* expression. (**B**) The *350dupA* mutation disrupts the binding of p63 to Motif1 and creates a repressive novel site for Lef1-βCat that interferes with the binding of p63 to the second Motif2 to significantly disrupt *IRF6* expression.

## DISCUSSION

Since mutations in the exons of *IRF6* accounted for only ~70% of VWS cases, we hypothesized that etiologic mutations would be found in regulatory elements near *IRF6*. While we sequenced the three most highly conserved regions near *IRF6*, we were most interested in *MCS9.7* because it is an enhancer element that replicates endogenous *IRF6* expression in critical tissues, and because it contains rs642961, a common DNA variant that is highly associated with non-syndromic CLP. Within the *MCS9.7* element, we found a new DNA mutation (*350dupA*) in a proband with VWS from a large Brazilian pedigree.

Although we found no other mutations within *MCS9.7* in 70 VWS cases, several lines of evidence suggest that this variant was etiologic. First, the DNA variant was found in all three affected members of this family that were tested. While the 350*dupA* was also found in two individuals who were not affected, it is known that the penetrance for VWS is not complete, even for deletion mutations (6). Second, the *350dupA* mutation was not found in any of the unaffected control individuals or in publicly available databases. We note, however, that this family originated in the South of Brazil and the control samples were limited in their geographic match. Third, the *350dupA* mutation disrupted *MCS9.7* enhancer activity in two different cell lines as well as *in vivo*, using a transgenic murine embryo assay. The *in vivo* results are particularly noteworthy because using a similar assay we failed to detect a disruption in enhancer activity when *MCS9.7* contained the risk allele of rs642961 (Supplementary Material, Fig. S1). Thus, our *in vitro* and *in vivo* data strongly support the hypothesis that the *350dupA* mutation is etiologic.

These data suggest a unique example where a mutation in an enhancer causes a human Mendelian disorder (25). While there are a few examples in the literature about gain-of-function mutations in regulatory elements that are associated with human genetic disorders, none of these regulatory mutations was characterized at the molecular level (20–23). One of these examples is the gain-of-function mutation in SHH enhancer (ZRS, zone of polarizing activity). These mutations led to development of preaxial polydactyly due to the ectopic expression in fore- and hindlimbs in transgenic murine embryos. However, the mechanism of ectopic regulation in limbs has not yet been determined (22,23). One possible explanation for the paucity of etiologic enhancer mutations is that genes have redundancy of both enhancers and of cis-binding sites within the enhancer (26,27). We do not know if there is redundancy for the *MCS9.7* enhancer element, but our previous study showed that p63 binds to two sites, Motif1 and Motif2, and both sites are required for full *MCS9.7* enhancer activity in primary human keratinocytes (11). In this study, a single mutation in Motif1 found in the Brazil family had the same effect on *MCS9.7* enhancer activity as *in vitro* mutations in both Motif1 and Motif2 in the earlier study. Our data are consistent with a two-step, loss-of-function and gain-of-function mechanism whereby the mutation directly abrogated binding to Motif1 and indirectly abrogated binding to Motif2 by creating a *de novo* binding site for a repressor transcription factor through an as yet uncharacterized mechanism (Fig. 6B). Indeed, we showed that the *350dupA* mutation created a binding site for the Lef1 transcription factor and showed that Lef1 is expressed in tissues where *MCS9.7* was shown previously to be active (Fig. 5A–C). However, it is possible that other transcription factors could bind to the *de novo* site created by the *350dupA* mutation and interferes with *MCS9.7* enhancer activity as an alternative mechanism for the pathological effect. Future studies are required to determine the repressive mechanism of Motif2 of p63.

These results are relevant to similar studies that identify and characterize regulatory mutations for Mendelian and non-Mendelian disorders. For VWS, our data were consistent with the hypothesis that the rare DNA variant at the cis-overlapping site in *MCS9.7* is etiologic for VWS, and supports the rationale for additional mutation screening of the *MCS9.7* enhancer element and other potential regulatory elements in patients with CLP (Fig. 6A). Our earlier study suggested that at least one other enhancer exists for *IRF6* because the *MCS9.7* enhancer is not active in the medial edge epithelium (MEE) during palatal fusion, even though *Irf6* is highly expressed in these cells (10). For example, a conserved element that is 2.4 kb upstream from the *IRF6* transcriptional start site had enhancer activity in human primary keratinocytes and was bound by activated Notch1 (28). These other *IRF6* enhancers also need to be sequenced in cases of isolated CLP because rs642961, the common DNA variant in *MCS9.7*, does not account for all of the risk at the *IRF6* locus, especially for cleft palate (9).

It is also interesting to compare and contrast the effects of rs642961 and *350dupA*. While the common mutation rs642961 abrogated the binding of TFAP2A to one of the cis motifs (9), *350dupA* mutation disrupted the binding of p63 to Motif1. However, only *350dupA* had a detectable effect on enhancer activity *in vivo*. At least three explanations are possible, (i) the derived allele for rs642961 is not the risk allele, but is in linkage disequilibrium with the real risk allele, (ii) the derived allele for rs642961 is the risk allele, and its effect can be detected at other time points, and (iii) the derived allele for rs642961 is the risk allele, but like other common alleles, its effect is small (29) and thus may not be detected by this assay. The comparison of these two regulatory variants is significant because 9 of 10 loci identified by genome-wide association studies for isolated CLP were mapped to intergenic regions (30–32).

Finally, these data highlight the important role of *IRF6* in oral epithelial tissues outside the MEE for proper development of the lip and palate. Previously, we showed that the highest level of *IRF6* expression is within the cells of the MEE during palatal fusion (33). However, we recently showed that the *MCS9.7* enhancer is not active in the MEE at this time in development (10). Thus, the identification of disease-associated DNA variants in *MCS9.7* along with its lack of activity in the MEE suggests that normal development of the lip and palate requires *IRF6* function in a cell type other than MEE. In support of this hypothesis, two recent papers point to the role of *Irf6* in periderm development as a critical process for development of the lip and palate (34,35).

## MATERIALS AND METHODS

### Pedigree and DNA sequencing

Informed consent was obtained from each individual that participated in this study. The IRB protocol approval was obtained from the University of Iowa for use of DNA samples from patients and control individuals. Permission was obtained to publish unidentifiable photos of affected individuals. In our previous study, we sequenced patients from 307 VWS families, the sequence analysis showed that only 70% of the affected families carry an exonic mutation within the *IRF6* gene (5,6). To test if non-coding variants could also result in VWS, we sequenced the probands from 70 VWS families without exonic mutations. For controls, we sequenced 100 unrelated individuals (70 from Iowa and 30 from Brazil) that lacked any history of orofacial clefting or any other birth defects. We sequenced three multi-species conserved sequences, *MCS9.7*, *IRF6-Intron2* and *IRF6-3′UTR*, as described previously (9). PCR products were sequenced using an ABI 3730XL (Functional Biosciences, Inc., Madison, WI, USA). Chromatograms were transferred to a UNIX workstation, base-called with PHRED (v. 0.961028), assembled with PHRAP (v. 0.960731), scanned by POLYPHRED (v. 0.970312) and viewed with the CONSED program (v. 4.0).

### Mapping of putative transcription factor binding sites

Transcription Element Search System (TESS, www.cbil.upenn.edu/tess) and JASPAR (www.jaspar.genereg.net) were used to predict putative transcription factor binding sites within the *MCS9.7* enhancer element (9). This element is 607 bp long and 9.7 kb upstream from the *IRF6* transcription start site. We used databases of mammalian and vertebrate transcription factor binding motifs for the prediction of putative binding sites. These sites were filtered based on spatial–temporal expression pattern in orofacial tissues during embryonic development (1,36).

### Cloning of MCS9.7 element and MCS9.7-350dupA

The *MCS9.7* wild-type allele was amplified from human genomic DNA (Clontech, Mountain View, CA, USA) using HiFi Platinum Taq (Invitrogen, CA, USA) and cloned into a pGL3-basic-*Luc*, pGL3-SV40p-*Luc*, pGL3-SV40-*Renilla*, Hsp68-promoter-*LacZ* reporter vector. The DNA sequence was verified by Sanger sequencing at the DNA Sequencing and Genotyping Core Laboratory at Michigan State University. Base pair changes present in the cloned amplicon were compared with the hg19 reference genome. Any changes were reverted to the reference allele using the QuickChange Lightning Multi Site-Directed Mutagenesis kit (Agilent Technologies, Santa Clara, CA, USA). The *350dupA* mutation, found in the patients from the Brazilian VWS pedigree, was introduced into the wild-type reference allele by site-directed mutagenesis. Prior to injection, both wild-type and *350dupA* constructs were linearized with XhoI and purified using Qiagen PCR purification Kit (Qiagen, Gaithersburg, MD, USA). Since the *350dupA* mutation was found in cis-overlapping motifs where the binding site of p63 Motif1 completely overlapped with Ebox3 and 4, we introduced insertions and substitutions to disrupt each binding site independently and in combination with test its role in *MCS9.7* activity.

### Cell culture and luciferase assay

For cell transfection, a 96-well plate with a glass bottom was used to grow HEK293 cells in medium that contained DMEM, 10% FBS and antibiotics at 37°C. HEK293 cells were used for transactivation experiments because they are biologically relevant (human, express *IRF6* and are epithelial) and they grow and transfect well. The cells were transfected 1 h after plating using lipofectamine 2000 (Invitrogen) with pGL3-basic-*Luc*, pGL3-*MCS9.7-Luc*, pGL3-*MCS9.7-350dupA-luc* and pGL3-*Lef1-βCatenin* (βCat). The pGL3-SV40-*Renilla* plasmid served as an internal control for transfection efficiency. The effect of overexpression of ΔNp63 on *MCS9.7* activity was also tested using the luciferase assay in osteosarcoma (Saos2) cells as previously described (11). Like HEK293 cells, Saos2 cells originate from human tissues are epithelial and transfect efficiently.

### Generation of transgenic mice

All procedures of this study involving animals were reviewed and approved by the Animal Welfare and Research Committee at Lawrence Berkeley National Laboratory. Transgenic murine embryos were generated by pronuclear injection for three constructs of *MCS9.7*; one that carries the common haplotype ('wild-type'), one that carries the *350dupA* allele (*MCS9.7-350dupA*) and one that carries the risk allele for rs642961 (*MCS9.7-rs642961A*). The *MCS9.7-rs642961A* construct was tested as previously described (9). To minimize experimental variation, all microinjections and embryo processing steps for the wild-type and *MCS9.7-350dupA* were done in parallel under identical conditions. Murine embryos were stained for 2.5 h at room temperature. Overall, a similar number of transgenic embryos were obtained from the wild-type (15/60 embryos) and *MCS9.7-350dupA* alleles (16/62 embryos) injections.

### EMSA

To test the effect of the *350dupA* mutation on binding of transcription factor proteins to *MCS9.7*, oligos were tagged with IR-700 at 5′ ends (IDT, Coralville, IA, USA). The EMSA assay was performed using the Li-COR binding mixture and a recombinant protein of interest as previously described (9). Sequence of oligos and primers used in this study is provided in Supplementary Material, Table S2.

### Chromatin immunoprecipitation (ChIP)-qPCR

To test the binding profile of transcription factors to *MCS9.7* enhancer element in cell culture, we performed ChIP followed by quantitative real-time PCR in human epithelial HEK293 cells. In addition, we used HaCaT cells because they originate from keratinocytes and express *IRF6*. We tested binding of p63 (sc-8344, Santa Cruz, CA, USA), E47 (sc-133074X, Santa Cruz, CA, USA), Hand2 (sc-22818X, Santa Cruz, CA, USA) and cMyc (sc-373712X, Santa Cruz, CA, USA) because *350dupA* mutation was mapped to cis-overlapping motifs of p63 and Ebox3/4. A non-conserved neighboring region that is 800 bp away from *MCS9.7* was used as an internal control for the efficiency of chromatin sheering and non-specific signal. The binding of PolII at the promoter region of the *IRF6* transcriptional start site was used to detect the transcriptional state of the gene. Promoter region of *PCNA* was used as a control for PolII constitutive binding (Supplementary Material, Fig. S2). To quantify the amount of immunoprecipitated DNA that has been pulled down by each transcription factor, we used SYBR Green Kit (Applied Biosystems, Foster City, CA, USA) to measure DNA amplification by an ABI 7500 real-time PCR machine. We included five replicates for each treatment, applied the standard curve method for quantifications and normalized the data to the level of immunoprecipitated DNA that was pulled down by H3 antibodies as previously described (9). Immunoprecipitated targeted DNA using null antibodies and IgG served as negative controls for background signal and non-specific binding.

### Immunostaining

For immunostaining, we followed the same protocol as previously described (10). The primary antibodies rabbit anti-Irf6 (SAB2102995, Sigma-Aldrich, MO, USA) and mouse anti-Lef1 (Ab12034, Abcam, MA, USA) were used. The secondary antibodies are, respectively, a goat anti-rabbit (A21429, Molecular Probes, CA, USA) and goat anti-mouse (A11029, Molecular Probes, CA, USA). We marked nuclei with DAPI (D3571, Invitrogen). An X-Cite Series 120Q laser and a CoolSnap HQ2 photometric camera are used to capture images from a Plan APO 40x/0.95 DIX M/N2 objective. NIS Elements Advanced Research v3.10 was used for RAW image deconvolution.

## SUPPLEMENTARY MATERIAL

Supplementary Material is available at *HMG* online.

## ACKNOWLEDGEMENTS

We would like to thank the many patients and family members and clinicians for participating in this study. We also thank Dr Brad Amendt for providing plasmids.

*Conflict of Interest statement*. None declared.

## FUNDING

Financial support for this research was provided for B.C.S. by NIH-DE13513 and Y.A.K. by F31DE022696. A.V. was supported by NIH/NIDCR FaceBase grant U01DE020060. C.A. was supported by a SNSF advanced researcher fellowship. Research by A.V. and C.A. was conducted at the E.O. Lawrence Berkeley National Laboratory and performed under Department of Energy Contract DE-AC02-05CH11231, University of California.

## REFERENCES

1. Dixon, M.J., Marazita, M.L., Beaty, T.H. and Murray, J.C. (2011) Cleft lip and palate: understanding genetic and environmental influences. *Nat. Rev. Genet.*, **12**, 167–178.
2. Kondo, S., Schutte, B.C., Richardson, R.J., Bjork, B.C., Knight, A.S., Watanabe, Y., Howard, E., de Lima, R.L., Daack-Hirsch, S., Sander, A. *et al.* (2002) Mutations in IRF6 cause Van der Woude and popliteal pterygium syndromes. *Nat. Genet.*, **32**, 285–289.
3. Zucchero, T.M., Cooper, M.E., Maher, B.S., Daack-Hirsch, S., Nepomuceno, B., Ribeiro, L., Caprau, D., Christensen, K., Suzuki, Y., Machida, J. *et al.* (2004) Interferon regulatory factor 6 (IRF6) gene variants and the risk of isolated cleft lip or palate. *N. Engl. J. Med.*, **351**, 769–780.
4. Burdick, A.B., Bixler, D. and Puckett, C.L. (1985) Genetic analysis in families with van der Woude syndrome. *J. Craniofac. Genet. Dev. Biol.*, **5**, 181–208.
5. de Lima, R.L., Hoper, S.A., Ghassibe, M., Cooper, M.E., Rorick, N.K., Kondo, S., Katz, L., Marazita, M.L., Compton, J., Bale, S. *et al.* (2009) Prevalence and nonrandom distribution of exonic mutations in interferon regulatory factor 6 in 307 families with Van der Woude syndrome and 37 families with popliteal pterygium syndrome. *Genet. Med.*, **11**, 241–247.
6. Leslie, E.J., Standley, J., Compton, J., Bale, S., Schutte, B.C. and Murray, J.C. (2012) Comparative analysis of IRF6 variants in families with Van der Woude syndrome and popliteal pterygium syndrome using public whole-exome databases. *Genet. Med.*, **141**, 1–7.
7. Koillinen, H., Wong, F.K., Rautio, J., Ollikainen, V., Karsten, A., Larson, O., Teh, B.T., Huggare, J., Lahermo, P., Larsson, C. *et al.* (2001) Mapping of the second locus for the Van der Woude syndrome to chromosome 1p34. *Eur. J. Hum. Genet.*, **9**, 747–752.
8. Osoegawa, K., Vessere, G.M., Utami, K.H., Mansilla, M.A., Johnson, M.K., Riley, B.M., L'Heureux, J., Pfundt, R., Staaf, J., van der Vliet, W.A. *et al.* (2008) Identification of novel candidate genes associated with cleft lip and palate using array comparative genomic hybridisation. *J. Med. Genet.*, **45**, 81–86.
9. Rahimov, F., Marazita, M.L., Visel, A., Cooper, M.E., Hitchler, M.J., Rubini, M., Domann, F.E., Govil, M., Christensen, K., Bille, C. *et al.* (2008) Disruption of an AP-2alpha binding site in an IRF6 enhancer is associated with cleft lip. *Nat. Genet.*, **40**, 1341–1347.
10. Fakhouri, W.D., Rhea, L., Du, T., Sweezer, E., Morrison, H., Fitzpatrick, D., Yang, B., Dunnwald, M. and Schutte, B.C. (2012) MCS9.7 enhancer activity is highly, but not completely, associated with expression of Irf6 and p63. *Dev. Dyn.*, **241**, 340–349.
11. Thomason, H.A., Zhou, H., Kouwenhoven, E.N., Dotto, G.P., Restivo, G., Nguyen, B.C., Little, H., Dixon, M.J., van Bokhoven, H. and Dixon, J. (2010) Cooperation between the transcription factors p63 and IRF6 is essential to prevent cleft palate in mice. *J. Clin. Invest.*, **120**, 1561–1569.
12. Thomason, H.A., Dixon, M.J. and Dixon, J. (2008) Facial clefting in Tp63 deficient mice results from altered Bmp4, Fgf8 and Shh signaling. *Dev. Biol.*, **321**, 273–282.
13. Celli, J., Duijf, P., Hamel, B.C., Bamshad, M., Kramer, B., Smits, A.P., Newbury-Ecob, R., Hennekam, R.C., Van Buggenhout, G., van Haeringen, A. *et al.* (1999) Heterozygous germline mutations in the p53 homolog p63 are the cause of EEC syndrome. *Cell*, **99**, 143–153.
14. Mills, A.A., Zheng, B., Wang, X.J., Vogel, H., Roop, D.R. and Bradley, A. (1999) p63 is a p53 homologue required for limb and epidermal morphogenesis. *Nature*, **398**, 708–713.
15. Yang, A., Zhu, Z., Kapranov, P., McKeon, F., Church, G.M., Gingeras, T.R. and Struhl, K. (2006) Relationships between p63 binding, DNA sequence, transcription activity, and biological function in human cells. *Mol. Cell.*, **24**, 593–602.
16. Zarnegar, B.J., Webster, D.E., Lopez-Pajares, V., Vander Stoep Hunt, B., Qu, K., Yan, K.J., Berk, D.R., Sen, G.L. and Khavari, P.A. (2012) Genomic profiling of a human organotypic model of AEC syndrome reveals ZNF750 as an essential downstream target of mutant TP63. *Am. J. Hum. Genet.*, **91**, 435–443.
17. Ferretti, E., Li, B., Zewdu, R., Wells, V., Hebert, J.M., Karner, C., Anderson, M.J., Williams, T., Dixon, J., Dixon, M.J. *et al.* (2011) A conserved Pbx-Wnt-p63-Irf6 regulatory module controls face morphogenesis by promoting epithelial apoptosis. *Dev. Cell*, **21**, 627–641.
18. Kouwenhoven, E.N., van Heeringen, S.J., Tena, J.J., Oti, M., Dutilh, B.E., Alonso, M.E., de la Calle-Mustienes, E., Smeenk, L., Rinne, T., Parsaulian, L. *et al.* (2010) Genome-wide profiling of p63 DNA-binding sites identifies an element that regulates gene expression during limb development in the 7q21 SHFM1 locus. *PLoS Genet.*, **6**, 1–15.
19. McDade, S.S., Henry, A.E., Pivato, G.P., Kozarewa, I., Mitsopoulos, C., Fenwick, K., Assiotis, I., Hakas, J., Zvelebil, M., Orr, N. *et al.* (2012) Genome-wide analysis of p63 binding sites identifies AP-2 factors as co-regulators of epidermal differentiation. *Nucleic Acids Res.*, **40**, 7190–7206.
20. Epstein, D.J. (2009) Cis-regulatory mutations in human disease. *Brief Funct. Genomic Proteomic*, **8**, 310–316.
21. Huang, L., Jolly, L.A., Willis-Owen, S., Gardner, A., Kumar, R., Douglas, E., Shoubridge, C., Wieczorek, D., Tzschach, A., Cohen, M. *et al.* (2012) A noncoding, regulatory mutation implicates HCFC1 in nonsyndromic intellectual disability. *Am. J. Hum. Genet.*, **91**, 694–702.
22. Lettice, L.A., Heaney, S.J., Purdie, L.A., Li, L., de Beer, P., Oostra, B.A., Goode, D., Elgar, G., Hill, R.E. and de Graaff, E. (2003) A long-range Shh enhancer regulates expression in the developing limb and fin and is associated with preaxial polydactyly. *Hum. Mol. Genet.*, **12**, 1725–1735.
23. Lettice, L.A., Hill, A.E., Devenney, P.S. and Hill, R.E. (2008) Point mutations in a distant sonic hedgehog cis-regulator generate a variable regulatory output responsible for preaxial polydactyly. *Hum. Mol. Genet.*, **17**, 978–985.
24. Kolly, C., Suter, M.M. and Muller, E.J. (2005) Proliferation, cell cycle exit, and onset of terminal differentiation in cultured keratinocytes: pre-programmed pathways in control of C-Myc and Notch1 prevail over extracellular calcium signals. *J. Invest. Dermatol.*, **124**, 1014–1025.
25. Visel, A., Rubin, E.M. and Pennacchio, L.A. (2009) Genomic views of distant-acting enhancers. *Nature*, **461**, 199–205.
26. Visel, A., Taher, L., Girgis, H., May, D., Golonzhka, O., Hoch, R.V., McKinsey, G.L., Pattabiraman, K., Silberberg, S.N., Blow, M.J. *et al.* (2013) A high-resolution enhancer atlas of the developing telencephalon. *Cell*, **152**, 895–908.
27. Perry, M.W., Boettiger, A.N. and Levine, M. (2011) Multiple enhancers ensure precision of gap gene-expression patterns in the Drosophila embryo. *Proc. Natl Acad. Sci. USA*, **108**, 13570–13575.
28. Restivo, G., Nguyen, B.C., Dziunycz, P., Ristorcelli, E., Ryan, R.J., Ozuysal, O.Y., Di Piazza, M., Radtke, F., Dixon, M.J., Hofbauer, G.F. *et al.* (2010) IRF6 is a mediator of Notch pro-differentiation and tumour suppressive function in keratinocytes. *EMBO J.*, **30**, 4571–4585.
29. Manolio, T.A., Collins, F.S., Cox, N.J., Goldstein, D.B., Hindorff, L.A., Hunter, D.J., McCarthy, M.I., Ramos, E.M., Cardon, L.R., Chakravarti, A. *et al.* (2009) Finding the missing heritability of complex diseases. *Nature*, **461**, 747–753.
30. Mangold, E., Ludwig, K.U., Birnbaum, S., Baluardo, C., Ferrian, M., Herms, S., Reutter, H., de Assis, N.A., Chawa, T.A., Mattheisen, M. *et al.* (2011) Genome-wide association study identifies two susceptibility loci for nonsyndromic cleft lip with or without cleft palate. *Nat. Genet.*, **42**, 24–26.
31. Birnbaum, S., Ludwig, K.U., Reutter, H., Herms, S., Steffens, M., Rubini, M., Baluardo, C., Ferrian, M., Almeida de Assis, N., Alblas, M.A. *et al.*

(2009) Key susceptibility locus for nonsyndromic cleft lip with or without cleft palate on chromosome 8q24. *Nat. Genet.*, **41**, 473–477.
32. Beaty, T.H., Murray, J.C., Marazita, M.L., Munger, R.G., Ruczinski, I., Hetmanski, J.B., Liang, K.Y., Wu, T., Murray, T., Fallin, M.D. *et al.* (2011) A genome-wide association study of cleft lip with and without cleft palate identifies risk variants near MAFB and ABCA4. *Nat. Genet.*, **42**, 525–529.
33. Knight, A.S., Schutte, B.C., Jiang, R. and Dixon, M.J. (2006) Developmental expression analysis of the mouse and chick orthologues of IRF6: the gene mutated in Van der Woude syndrome. *Dev. Dyn.*, **235**, 1441–1447.
34. Richardson, R.J., Dixon, J., Jiang, R. and Dixon, M.J. (2009) Integration of IRF6 and Jagged2 signalling is essential for controlling palatal adhesion and fusion competence. *Hum. Mol. Genet.*, **18**, 2632–2642.
35. de la Garza, G., Schleiffarth, J.R., Dunnwald, M., Mankad, A., Weirather, J.L., Bonde, G., Butcher, S., Mansour, T., Kousa, Y.A., Fukazawa, C.F. *et al.* (2012) Interferon Regulatory Factor 6 promotes differentiation of the periderm by activating expression of grainyhead-like 3. *J. Invest. Dermatol.*, **133**, 68–77.
36. Jugessur, A., Farlie, P.G. and Kilpatrick, N. (2009) The genetics of isolated orofacial clefts: from genotypes to subphenotypes. *Oral Dis.*, **15**, 437–453.